Supporting Information

Polymer-laden Composite Lignin-based Electrolyte Membrane for High Performance Lithium Batteries

Shi Wang[†a], Lei Zhang[†b], Ailian Wang[a], Xu Liu[a], Jie Chen[a], Zhinan Wang[a], Qinghui Zeng[a], Heng-hui Zhou,[c] Xiaorui Jiang,[d]* Liaoyun Zhang[a]*

[a] *School of Chemical Sciences, University of Chinese Academy of Sciences, 19 Yuquan Road, Shijingshan District, Beijing 100049, China*

[b] *College of Science, China University of Petroleum-Beijing (CUPB), 18 fuxue road, Changping District, Beijing 102249, China*

[c] *College of Chemistry and Molecular Engineering, Peking University, 5 Yiheyuan Road, Haidian District, Beijing 100871, China*

[d] *Pulead Technology Industry Co., Ltd, No.35 Innovation Road, Science Park, Changping District, Beijing 102200, China.*

[†] *Shi Wang and Lei Zhang contributed equally to this work.*

**E-mails: zhangly@ucas.ac.cn; jiangxiaorui@pulead.com.cn*

Contents

Pages: 13; Figures: 6; Tables: 5

Materials

Vinylimidazole (VIm, 99 %, Aladdin), organic liquid electrolyte (TC-E201, EC/DMC/EMC, Guangzhou Tinci Materials Technology Co., Ltd.), commercial separator (Celgard2300) and poly(ethylene glycol) methyl ether methacrylate (PEGMA, M_n = 950 g mol^{-1}, Aldrich) were used as received. Toluene was purchased from Beijing Chemical Works and dried with CaH_2, and distilled before use. Azoisobutyronitrile (99%, AIBN, Aladdin, China) was alternantly recrystallized from diethyl ether (AR, Beijing Chemical Works) and methanol (AR, Beijing Chemical Works) before use. Lignin (Hebei qingjun cellulose plant) was dried at 80 °C for 24 h before use.

Characterization

Fourier transform infrared spectroscopy (FTIR, Thermo Nicolet AVATAR 360 infrared instrument with an attenuated total reflectance (ATR) attachment) was used to obtain the infrared spectra (IR) of the samples from 4000 to 500 cm^{-1}. Raman spectra of lignin-based electrolyte and liquid electrolyte were collected by Raman analysis (532 nm, Renishaw in Via). Thermal stability analyses were measured on a thermo gravimetric analyzer from 50 to 600 °C using a thermal gravimetric analysis (Perkin–Elmer TGA 1 series instrument) with a heating rate of 20 °C min^{-1} under nitrogen atmosphere. ^{1}H NMR spectrum of the LCP was obtained on a JNM-ECZ400S (JEOL, 400 MHz) spectrometer at RT using DMSO as the solvent (TMS as the internal standard). Gel permeation chromatography (GPC) measurement of the LCP was performed using a PL-GPC50 equipped with a refractive index detector at 40 °C (polystyrene used as the standard and DMF used as the eluent with a flow rate of 1.0 mL min^{-1}). The surface morphology of the pure lignin, lignin-based film and lithium metal was observed by Field Emission Scanning Electron Microscope (FESEM, Hitachi SU8010). The pure lignin and lignin-based film for SEM were sputtered with Au for 30 s. The stress-strain measurement was done to test the mechanical property of the lignin-based film with universal testing system (Instron5900) at a tensile speed of 2 mm min^{-1}.

Electrochemical measurements

The ionic conductivity of the lignin-based electrolyte film was tested by AC impedance spectroscopy (using a ZahnerEnnium electrochemical workstation) with a frequency range from 1 Hz to 1 MHz, AC amplitude of 5 mV, and temperature range from 30 to 80 °C via the two-probe method. The lignin-based film was dipped in the electrolyte for ~5 s (the film was also activated in the same way for all the other electrochemical tests). Then, the film was sealed between two stainless steel plates for ionic conductivity tests. The samples were held at each temperature for 30 min before testing. Then, the ionic conductivity was calculated by

$$\sigma = \frac{L}{SR} \quad \text{(S1)}$$

Where R is the bulk resistance of the film, S is the contact area of the film and electrode, and L is the thickness of electrolyte films.

The electrochemical stability window of lignin-based electrolyte film was measured by the ZahnerEnnium electrochemical workstation with a Li metal/lignin-based electrolyte/stainless steel coin cell, the linear sweep voltammogram was tested from 0.5 to 5.5 V (vs. Li^+/Li) at a scan rate of 5 mV s^{-1} at 30 °C.

To measure the lithium-ion transference number (t^+) of the lignin-based electrolyte membrane, the AC impedance plots of a symmetric Li/electrolyte/Li cell was measured before and after DC polarization at 30 °C. Subsequently, the t^+ was calculated using Equation (S2).

$$t_{Li}^{+} = \frac{I_s(\Delta V - I_0 R_{lo})}{I_0(\Delta V - I_s R_{ls})} \quad \text{(S2)}$$

Where I_o and I_s are the initial and steady state current, respectively. They were measured by DC polarization with a voltage (ΔV = 10 mV). In addition, R_{lo} and R_{ls} are the initial and steady interfacial resistances (Ω), respectively, which were obtained before and after polarization from the impedance spectra of the cell (oscillation voltage of 5 mV, frequency between 100 mHz and 1 MHz).

Interfacial compatibility was conducted by monitoring the interfacial resistance of the Li/lignin-based electrolyte/Li cell at 30 °C at different aging times. The measurement

was carried out on the ZahnerEnnium electrochemical workstation with an oscillation voltage of 5 mV in the frequency range from 100 mHz to 1 MHz.

$LiFePO_4$ (LFP)/lignin-based electrolyte/Li and $LiCoO_2$ (LCO)//lignin-based electrolyte/Li cells were assembled to evaluate the cell performances of the lignin-based electrolyte. The LFP/separator-organic electrolyte/Li cell was also assembled and tested as comparison at the same condition. The process was performed in an Ar-filled glovebox (MB-Labstar 1200/780) with H_2O and O_2 contents below 0.5 ppm. The LFP-based cathode consisted of 70 wt% LFP (Pulead Technology Industry Co., Ltd, China), 20 wt% super P and 10 wt% binder (PVDF). The LCO-based cathode consisted of 90% LCO (Pulead Technology Industry Co., Ltd, China), 5% super P and 5% binder (PVDF). The charge and discharge cycles of the LFP-based cell (the potential range between 2.5 and 4.0 V) and LCO-based cells (the potential range between 3 and 4.3 V) were carried out on LANHE CT2001A battery testing system at room temperature (RT).

Lithium plating/striping experiments for the lignin-based electrolyte membrane and the separator-liquid electrolyte in a symmetric lithium coin cell were cycled at a current density of 1 mA cm^{-2} at RT. Both the charge and discharge times are 1 h.

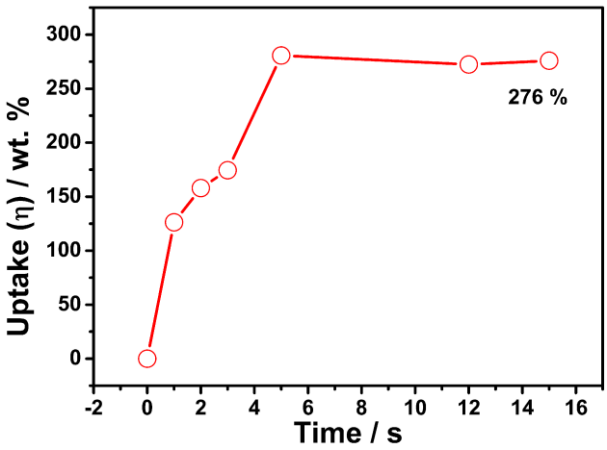

Figure S1. The liquid electrolyte uptake ability of lignin-based free-standing film depends on time.

The lignin-based film was dipped into organic liquid electrolyte. The liquid electrolyte adsorbing capacity (η) can be calculated by equation (S1):

$$\eta = \frac{w_2 - w_1}{w_1} \times 100\% \quad \text{(S3)}$$

Where w_2 and w_1 represent the weight of the lignin-based film after and before immersed into the organic liquid electrolyte, respectively.

As shown in Figure S3, the lignin-based film can uptake liquid electrolyte up to 276 %, indicating the superior adsorbing ability of the lignin-based film. Specifically, Before 5 s, the uptake contents of liquid electrolyte sharply increase, then, the uptake contents are kept almost constant.

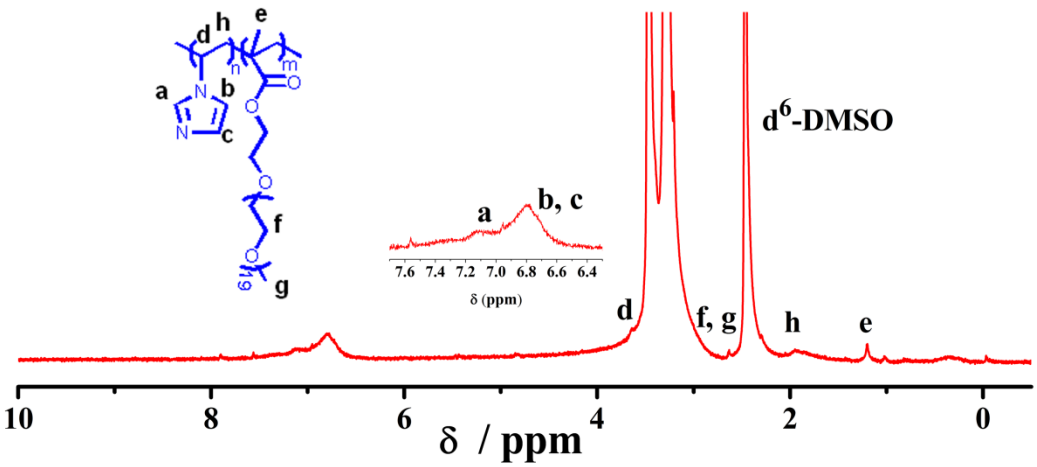

Figure S2. ^{1}H NMR spectrum of the LCP (PVIM-co-PPEGMA).

The structure information of the LCP (M_n = 4.56×10^4 g mol^{-1}, see Table S1) was characterized by ^{1}H NMR. As presented in Figure S1, the peaks ranging from 6.81 ppm to 7.16 ppm are attributed to the proton signals from the imidazole structure. Proton signals at 3.24, 3.35 and 3.51 ppm are assigned to the characteristic peaks from -O-CH_3(g), -O-CH_2-CH_2-O-(f) and -CH-N-(d), respectively. Thus, GPC, ^{1}H NMR and IR (Figure 1b) characterizations demonstrate that the LCP has been successfully synthesized.

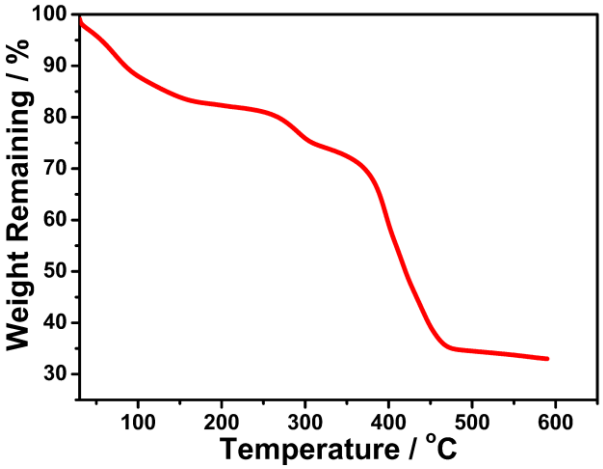

Figure S3. TGA curve of lignin-based electrolyte film.

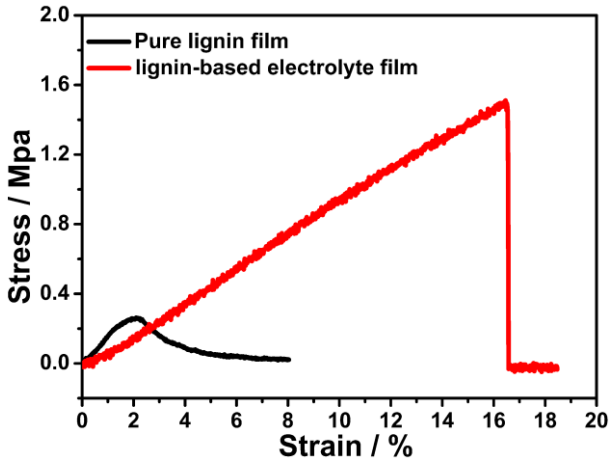

Figure S4. The stress-strain curves of pure lignin film and lignin-based composite electrolyte film.

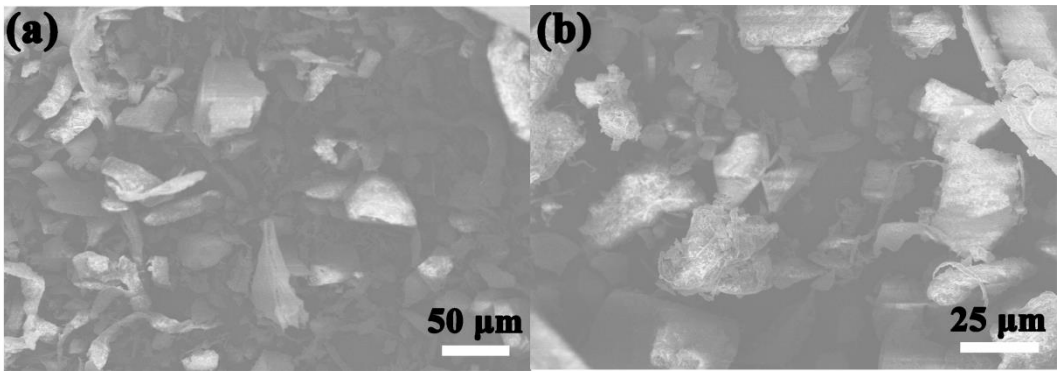

Figure S5. (a) and (b) show the SEM images of pure lignin at different magnifications.

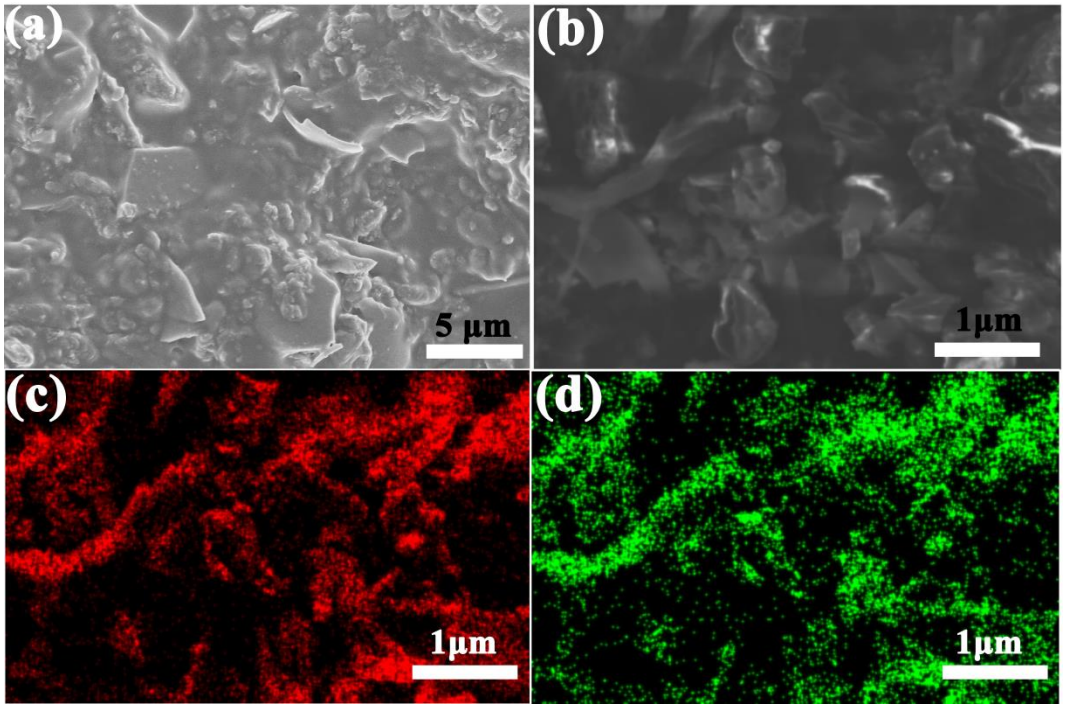

Figure S6. (a) SEM image of lignin-based composite film. (b) SEM image of the composite film and the corresponding elements mapping (c and d are the O element mapping and N element mapping, respectively) of the lignin-based film.

To further confirm lignin is uniformly coated by the LCP, SEM images at higher magnifications and the corresponding elements mapping of O and N are shown in Figure S6. In Figure S6a, it is clearly seen that lignin is uniformly coated by the LCP. Figure S6b is the SEM image used to obtain the elements mapping (O, N) of the composite film. Figure S6c shows the O element mapping of the composite film. Especially, the N element mapping in Figure S6d further demonstrates that lignin is uniformly coated by the LCP (the LCP contains N element while lignin is not).

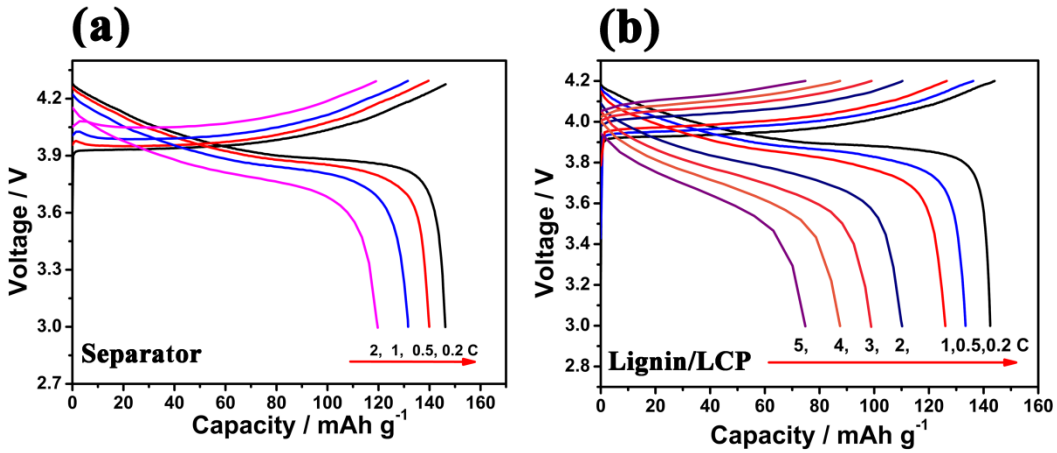

Figure S7. (a) and (b) show the charge and discharge curves of LCO/Li cell using separator-liquid electrolyte and lignin-based electrolyte, respectively.

Table S1. The related parameters and the molecular weight of the LCP.

Polymer	M_n / g mol^{-1}	M_w / g mol^{-1}	PDI
PVIM-*co*-PPEGMA (LCP)	4.56×10^4	5.16×10^4	1.2

Table S2. The related parameters *A*, E_a and T_o, which is obtained by a linear fitting on the experimental data.

Sample	*A*/ (S^{-1} cm^{-1} K$^{-1/2}$)	E_a / kJ mol^{-1}	R-square
Lignin-based electrolyte	0.5	7.24	0.97

Table S3. Fitting results of EIS analysis for Li/lignin-based electrolyte/Li cell (before and after polarization).

	R_1 (Ω)	R_2 (Ω)	*CPE1-T (F)*	*CPE1-P*	R_3(Ω)	*CPE2-T(F)*	*CPE2-P*
Before	8.552	84.09	8.6341×10^{-6}	0.83159	26.67	0.0033686	0.76728
After	8.736	82.3	8.0952×10^{-6}	0.83931	26.8	0.0032101	0.76518

Table S4. The related parameters and t^+ of the lignin-based electrolyte membrane.

Samples	R_{lo} (Ω)	R_{ls} (Ω)	I_o (μA)	I_s (μA)	t_{Li}^+
DLCCSPE-1000-8-UA	85	85	81.6	69.0	0.63

Table S5. Fitting results of EIS analysis for Li/lignin-based electrolyte/Li cell after different storage times.

Storage times	R_1 (Ω)	R_2 (Ω)	*CPE1-T(F)*	*CPE1-P*	R_3(Ω)	*CPE2-T(F)*	*CPE2-P*
Day 1	11.43	66.25	7.2209×10^{-6}	0.83244	50.72	0.0023788	0.69387
Day 2	7.316	75.12	1.1554×10^{-5}	0.78327	41.61	0.0020387	0.80187
Day 6	4.212	112.5	1.226×10^{-5}	0.76893	66.84	0.0017638	0.79092
Day 9	4.631	93.41	1.2586×10^{-5}	0.7698	50.29	0.0018096	0.81771
Day 10	3.77	83.71	1.1095×10^{-5}	0.7849	47.76	0.00211	0.76903
Day 11	8.571	86.06	1.3932×10^{-5}	0.76278	46.3	0.0021861	0.80473
Day 14	3.802	93.34	1.1608×10^{-5}	0.77571	53.38	0.0024281	0.74685
Day 20	4.605	79.14	1.1212×10^{-5}	0.78176	49.6	0.0030853	0.70154
Day 30	4.667	69.41	1.2482×10^{-5}	0.76951	35.38	0.0041276	0.72477